

# Thermomechanical Formation of Nanoscale Polymer Indents With a Heated Silicon Tip

William P. King

Woodruff School of Mechanical Engineering,

Georgia Institute of Technology,

Atlanta, GA 30332-0405

e-mail: william.king@me.gatech.edu

Kenneth E. Goodson

Department of Mechanical Engineering,

Stanford University,

Stanford, CA 94305-3030

*In thermomechanical data storage, a heated atomic force microscope cantilever tip is in contact with and scans over a polymer film. Heating in the cantilever and cantilever tip induces local deformation of the polymer near the tip, with indents as small as 22 nm. This paper reports a simple modeling approach for predicting heat and mass transfer in the cantilever tip and polymer with the goal of predicting indent formation conditions. The model accounts for subcontinuum conduction in the cantilever tip and for the time- and temperature-dependent mechanical properties of the polymer. Simulations predict steady state and transient indent formation, and the results compare well with data. For loading forces 30–200 nN and a tip radius of 20 nm, a cantilever temperature of 200°C is required to form an indent at steady state. For heating pulses as short as 5 μs, the cantilever temperature required for bit formation is as high as 500°C. By quantifying the conditions required for indent formation, this work may improve the operation of heated probes for thermomechanical data storage. [DOI: 10.1115/1.2764088]*

## Introduction

In thermomechanical data storage [1–3], a heated atomic force microscope (AFM) cantilever tip locally melts and deforms a polymer layer to form nanometer-scale data bits. Figure 1 illustrates this technology, in which critical figures of merit are data bit density and the time and temperature required to write data bits. This paper reports a simple modeling approach to predict heat transfer in the nanoscale silicon probe tip and the polymer layer during thermomechanical indentation formation.

Thermomechanical data storage technology has a spatial resolution and writing rate that are governed by heat transfer in the cantilever tip. Past work investigated thermal conduction within the cantilever with the goal of minimizing the time required for temperature changes near the tip region [4]. Research on high-resolution thermal microscopy motivated several studies of thermal and thermoelectric transport at the contact of a probe tip and a surface [5–8]. However, no previous work considered thermal conduction in a silicon AFM cantilever tip or its interaction with a polymer layer.

Previous published work on thermomechanical data storage noted the temperature, time, and loading force required to form a data bit but did not examine the process of data bit writing in detail. Previous studies [3,9] found a minimum temperature of 350°C in the cantilever heater region required to form indents in

thin layers of polymethyl methacrylate (PMMA). The temperature of the cantilever heater region can be found by measuring the electrical resistance of the cantilever, which is a function of temperature [10]. The minimum writing temperature of 350°C is higher than the glass transition temperature of PMMA, which is 100–120°C [11]. It is not well understood why the cantilever heater temperature must significantly exceed the polymer glass transition temperature in order to form an indent.

This paper considers thermal conduction along the cantilever tip in steady contact with the polymer to find the temperature distribution along the length of the cantilever and the temperature at the tip-polymer interface. The analysis also considers the melting of the polymer and motion of the tip into the polymer to predict indentation formation conditions.

## Technical Approach

The most rigorous study of heat conduction in the cantilever tip would provide a detailed account for phonon dispersion, and scattering on the tip walls and other phonons [12]. Several unknown experimental parameters mitigate the practical impact of the most rigorous approach. These include the presence of native silicon oxide on the tip, uncertainty in the tip shape, tip wear, and the evolution of these parameters over long times and temperatures. The degree of thermal conductivity anisotropy in the polymer layer is not known, and the surface tension and viscoelastic properties at length scales comparable near the polymer radius of gyration have not been measured, nor do good physical models exist for their prediction. This study employs an approximate model of phonon transport in the cantilever tip. Because the uncertainties in the experimental parameters are large compared to the uncertainty in the chosen model, a more rigorous model may not yield useful insight without advancement in the related experiments.

Figure 2 shows thermal conduction resistances in the cantilever tip and polymer substrate. Heat flows from the cantilever into the substrate across the air gap and through the cantilever tip. The thermal resistance across the air gap between the cantilever and the substrate is  $R_{\text{substrate}}$  and calculated from a shape factor [13]. The total thermal conduction resistance along the length of the cantilever tip is

$$R_{\text{tot}} = \int_{x=0}^h \frac{4x}{\pi d^2 k(x)} dx + \frac{16}{C \nu \pi d_{\text{contact}}^2} + R_{\text{substrate}} \quad (1)$$

where the first term is  $R_{\text{tip}}$ , the thermal conduction resistance along the  $x$  direction, the second term is the thermal interface resistance  $R_{\text{interface}}$  that enforces a phonon scattering site at the tip-polymer interface, and the third term is  $R_{\text{spread}}$ , the thermal resistance due to the spread of heat in the polymer layer. Note that  $R_{\text{spread}}$  is the thermal resistance to heat flow from the end of the tip, while  $R_{\text{substrate}}$  is the thermal resistance to heat flow from the cantilever heater region. The interface thermal resistance is thus calculated by enforcing that all of the available phonons scatter at the tip-polymer interface [14], and  $R_{\text{interface}}$  is typically  $10^6$ – $10^8$  K/W. The value of  $R_{\text{spread}}$  is typically  $10^8$ – $10^9$  K/W, found from solution to the heat conduction equation in the polymer layer.

The tip is modeled as a half-sphere mounted onto the end of a cone. The conduction analysis divides the tip into finite volume elements. The resistance to heat flow away from the tip is much greater than the resistance to heat flow within the tip, and thus the temperature along the tip can be analyzed as a one-dimensional problem. Thermal conduction is calculated between adjacent volume elements in the tip, conduction to the nearby air, and radiation to the nearby surfaces. The thermal conductivity in the tip is calculated using Matthiessen's rule [15,16].

Contributed by the Heat Transfer Division of ASME for publication in the JOURNAL OF HEAT TRANSFER. Manuscript received February 15, 2006; final manuscript received January 15, 2007. Review conducted by Suresh V. Garimella.

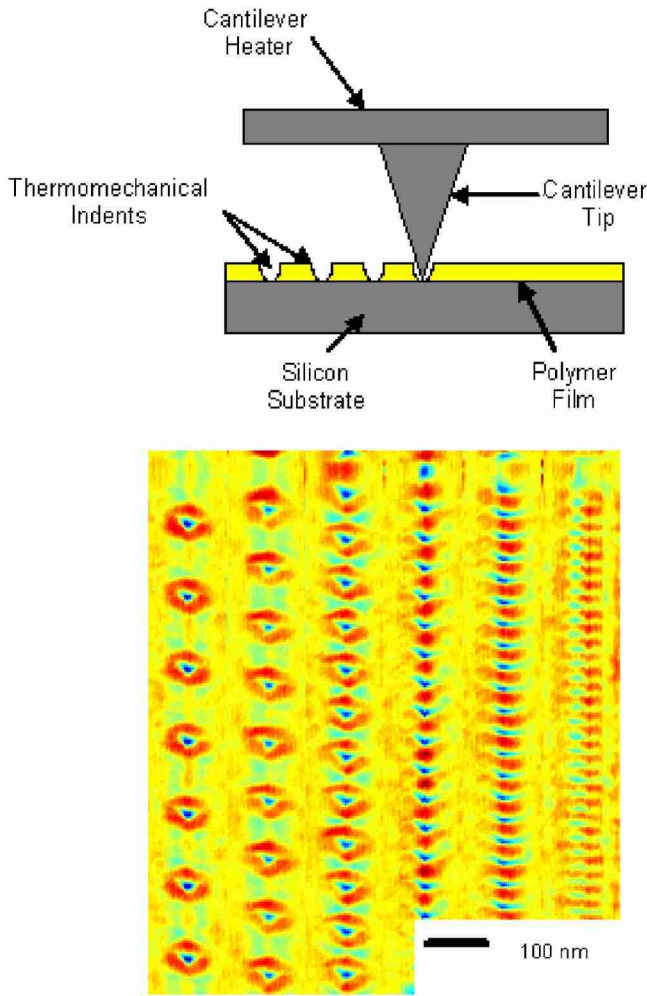


Fig. 1 Schematic of the bit-writing process and thermomechanically written indentations in polymer

$$k(x) = \frac{1}{3} C v \left[ \frac{1}{\Lambda^{-1} + d(x)^{-1}} \right] \quad (2)$$

where  $x$  is the vertical position along the tip,  $d$  is the local tip diameter,  $k$  is the local thermal conductivity of the tip,  $C$  is the volumetric heat capacity,  $v$  is the average phonon speed, and  $\Lambda$  is the phonon mean free path in the bulk material [15]. A value of  $1.8 \times 10^9 \text{ W/m}^2 \text{ K}$  is used for the product  $Cv$  [17]. The model assumes constant  $Cv$ , which will produce an error of not more than 15%. The temperature dependence of the bulk thermal conductivity of silicon is modeled using a fit to room temperature data for bulk samples [18], and so  $\Lambda$  is a function of temperature.

Typical tip loading forces are in the range of 5–300 nN [3,9] and so adhesive forces can be neglected [19]. While the PMMA polymer data layer is relatively hard with Young's modulus of  $3.0 \times 10^9 \text{ Pa}$  [11], it is much softer than the silicon tip and elastically deforms when unheated. An exact solution [20] is available for the indentation of a half-sphere into a nonadhering elastic surface, which relates the loading force  $F_{\text{load}}$  to the contact conditions

$$F_{\text{load}} = \frac{G'}{1 - \chi} \left[ (r_{\text{contact}}^2 + r_{\text{tip}}^2) \log \left( \frac{r_{\text{tip}} + r_{\text{contact}}}{r_{\text{tip}} - r_{\text{contact}}} \right) - r_{\text{tip}} r_{\text{contact}} \right] \quad (3)$$

where  $G'$  is the elastic modulus,  $r_{\text{contact}}$  is the radius of contact and half the value of  $d_{\text{contact}}$ , and  $r_{\text{tip}}$  is the tip radius of curvature.

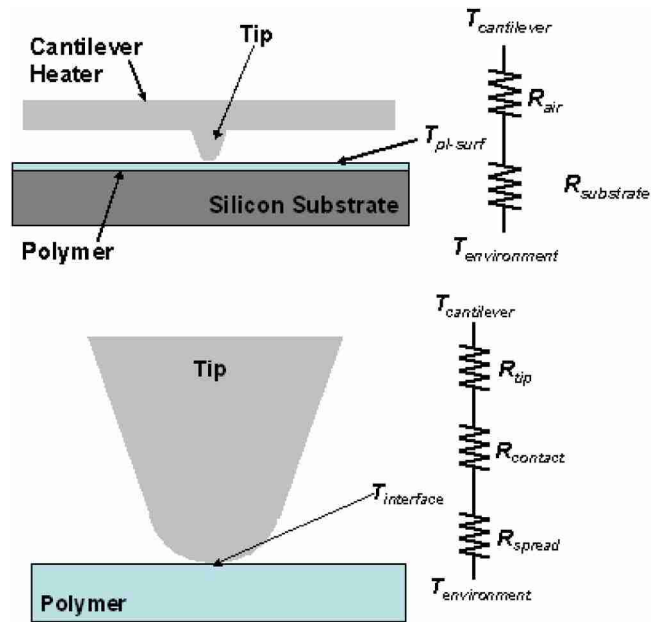


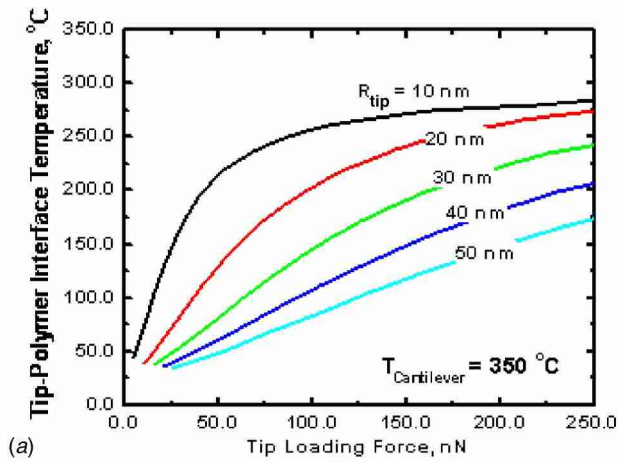
Fig. 2 Thermal resistance network showing the heat transfer modes influencing tip-sample interface temperature

Poisson's ratio is  $\chi=0.35$  for PMMA at room temperature. Once the polymer is heated above its glass transition point, it can be considered to be incompressible with  $\chi=0.5$  [11]. The thermal resistance of the portion of the tip that penetrates into the polymer is neglected, as the thermal resistance of the polymer is significantly greater than the thermal resistance of the tip.

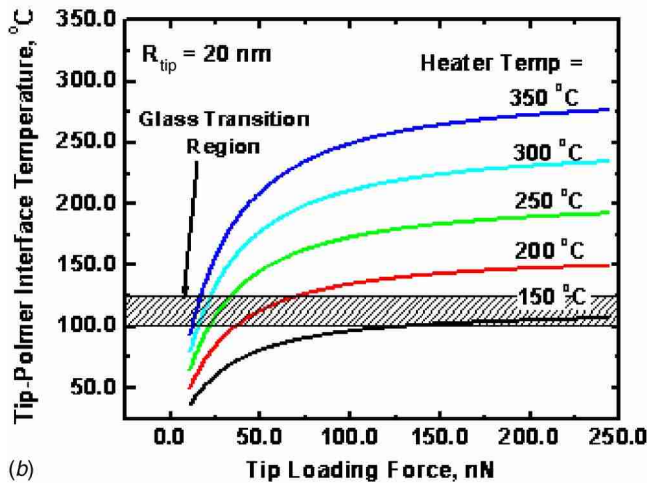
Heat flows from the side of the tip through radiative exchange with the heater and the substrate and conduction to the surrounding air. This steady-state model assumes that conduction across the cantilever-polymer air gap produces a constant, linear temperature gradient across the gap. Typical heating times are 1–50  $\mu\text{s}$  [4,21] which are much longer than the time for heat to diffuse across a typical cantilever-substrate air gap of thickness 0.3–1  $\mu\text{m}$  which is approximately 100 ns. Thus, the air between the cantilever and substrate is at thermal steady state. The resistance to thermal conduction between the tip and the air depends only on the Knudsen slip resistance, which accounts for the diameter of the tip being smaller than the mean free path of the air molecules [13,22].

The tip is discretized into 1000 volume elements along its axis, and the temperature distribution is found using Gauss-Seidel iteration on the heat flow along the length of the tip. Temperature predictions are validated by an energy balance on each volume element and on the entire tip, and compare well with analytical solutions in which the thermal conductivity is held constant. The calculated value of  $R_{\text{spread}}$  compares well with a shape factor for a disk source on an infinite half-space [22]. For transient analysis, time steps of 1% of the total simulation time yield a numerical solution that agrees to within 2% of the analytical solution for constant-temperature boundary conditions in both radial and normal directions.

A comparison of the heat conduction paths along the cantilever tip and across the air gap finds that the temperature at the tip-polymer interface  $T_{\text{interface}}$  is much higher than the temperature at the polymer surface away from the tip  $T_{\text{pl-surf}}$ . Because the temperature at the tip-polymer interface is much higher than the temperature anywhere else on the substrate surface, the cantilever might be used as a tool for highly local thermal processing or manufacturing [23,24]. Comparison of heat flow through the tip and across the air gap separating heater and polymer shows that significantly more heat travels across the cantilever-substrate air



(a)



(b)

**Fig. 3 Predicted steady-state tip-polymer interface temperature as a function of loading force for a range of heater temperatures and a tip radius of curvature of 20 nm. The shaded region represents the glass transition region, above which a bit will be written for long heating pulses.**

gap than travels through the length of the cantilever tip. Thus, it is the thermal impedance of the cantilever-substrate air gap not the thermal impedance at the cantilever tip-polymer interface, which governs thermal data reading [13,25,26].

Figure 3 shows the effect of loading force on interface temperature. The tip loading force influences the area of tip-polymer contact, which in turn affects the interface temperature. For the smallest tip radii, the tip-polymer interface temperature is relatively close to the cantilever heater temperature. However, as the tip sharpness decreases, the tip-polymer interface temperature decreases dramatically. For indents written into PMMA films, the PMMA has a glass transition temperature in the range of 100–125 °C, also shown in Fig. 3.

By coupling the mechanical and thermal analysis of bit formation, it is possible to predict the onset of data bit formation and the ultimate data bit size for a given heater temperature, heating time, and loading force. In the measurements reported on thermomechanical writing [1,3,27], the cantilever has a tip of height of 500 nm, tip radius of curvature of 20 nm, spring constant near 0.05 N/m, and a mechanical resonance frequency near 100 kHz. The polymer data substrate is a bilayer consisting of 35 nm of PMMA on 80 nm of epoxy, which resides on a silicon substrate. In the writing experiments, a cold cantilever tip is brought into contact with a cold polymer surface. After tip-polymer contact, the base of the cantilever is brought closer to the substrate such

that the cantilever tip is pressed into the substrate. The cantilever tip loading force  $F_{load}$  is the product of this displacement and the cantilever spring constant  $k$ . The cantilever heats for a fixed time to a known temperature.

The temperature-dependent mechanical modulus of the polymer is calculated as a function of temperature, pressure, and time. The temperature dependence takes the form of the Williams Landel Ferry shift parameter [28], which is used to extract viscous and elastic polymer properties from tabulated values [29]. For times comparable to and longer than 10 ms, the cantilever is in thermal and mechanical equilibrium with the polymer data layer. Figure 3 shows predictions for the tip-polymer interface temperature as a function of loading force for various heater temperatures. The model predicts that the lowest heater temperature at which a bit could be written is near 200 °C for a loading force above approximately 75 nN.

The cantilever motion of the cantilever tip can be described through an equation of motion

$$m_{cant}\ddot{x} + k_{cant}x = F_{load} - F_{pl} \quad (4)$$

where  $m_{cant}$  is the mass of the cantilever calculated as in previous work [3,9],  $x$  is the vertical position of the cantilever tip, and  $F_{pl}$  is the force with which the polymer resists tip motion. The force with which the polymer resists tip motion is a function of the temperature field in the polymer near the tip.

Solution of the two-dimensional transient diffusion equation within the polymer show that for all of the present calculations, the thickness of the softened polymer is thinner than the tip radius of curvature. The tip motion through the polymer can thus be modeled as a lubrication problem, where the viscoelastic polymer is squeezed between the hardened tip and the hard, cool polymer. An analytical solution for the force required to displace the lubrication layer links the tip motion to polymer relaxation. At every time step, the simulation tests whether the tip loading force is sufficient to move the tip one finite volume element thickness into the polymer layer. The force with which the polymer resists tip penetration  $F_{pl}$  can be divided into the viscous resistance [30] and the elastic resistance of the polymer [28]

$$F_{pl} = 3\pi \frac{\eta_{pl} r_{tip}^4}{t_{pl}^3} \dot{x} + 3\pi G' r_{tip}^2 \varepsilon \quad (5)$$

where  $\eta_{pl}$  is the polymer viscosity,  $t_{pl}$  is the average thickness of the softened polymer near the tip, and  $\varepsilon$  is the strain in the melted polymer. If the criteria for tip motion are met, then the tip moves one element into the polymer. The new position of the tip serves as a position of the constant-temperature boundary in the solution of the heat equation. Since the tip penetration is limited by the squeeze flow of the soft polymer between the tip and the hard polymer beneath, once the polymer flows away from the tip, it exerts negligible force on the tip. The simulation stops when the tip has penetrated to a depth of 10 nm.

Figure 4 shows measurement and prediction results for writing conditions required to form an indent for tip loading forces of 30–100 nN. The measurements are from Refs. [1,27]. Predictions from the modeling of the present study are shown for both a moving tip and for steady-state thermal conditions. To within experimental error and measurement scatter, the modeling and simulation of the present work compare well with measurements.

The drop in threshold writing temperature for longer writing times is due to three factors: the inertia of the cantilever which must be overcome for tip motion, heat diffusion into the polymer, and the viscoelastic response of the polymer to tip penetration. First, the cantilever mechanical time constant prohibits a data bit from being written much faster than approximately 10  $\mu$ s, so due only to the cantilever mechanical time constant, one expects an asymptotic increase in threshold writing temperature as heating times decrease to near 1  $\mu$ s. The steep increase in temperature required to write a data bit for short times also corresponds to the time required for heat to diffuse into the polymer layer away from

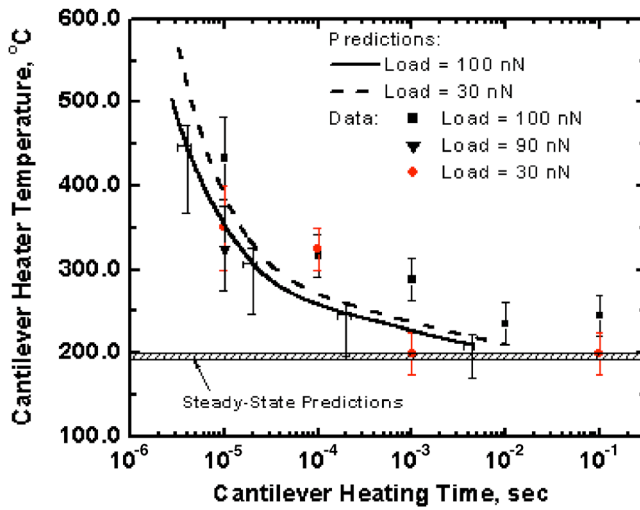


**Fig. 4 Prediction of the threshold conditions of time, temperature, and tip loading force required to produce a data bit for a 20 nm tip radius of curvature. The predictions compare well with data. The gray area shows predictions for near-equilibrium conditions.**

the tip, and the time- and temperature-dependences of the polymer properties away from the tip. As shown in Eq. (5), the force with which the polymer resists tip penetration has an inverse cubic dependence on the thickness of the soft polymer near the penetrating tip. The long time behavior of tip penetration, which asymptotically approaches a threshold bit-writing temperature of approximately 200°C, is a function of only the polymer temperature-dependent shear modulus.

The two loadings for which predictions are made bound the reasonable practical loading window of the present thermomechanical data storage cantilever. The large experimental scatter can be attributed to the difficulty of calibrating the cantilever heating temperature and loading force, as well as the difficulty of accurately measuring features of size near 10 nm. The predictions show a 20–50°C difference in threshold writing temperature between the 30 nN and 100 nN loading forces at a given heating time.

Figure 4 provides insight into the previously published experimental results that a threshold temperature of 350°C writes a data bit [5,14]. One possible explanation is that, as shown in Fig. 3, 350°C is the temperature at which a bit is *always* written, regardless of loading force. Another important parameter is that these reports always wrote bits at 10–20  $\mu$ s, for which the predictions of Fig. 4 show that the threshold writing temperature is 300–350°C.

The shape of the cantilever tip can impact the onset writing conditions. Previous work has shown that an AFM tip can wear over time [31,32]. The limits of data density in a thermomechanical data storage system depend on the sharpness of the cantilever tip, and thus it is desirable to reduce the wear of the tip as much as possible. The tip shape affects not only the size of the ultimate bit but also the time and temperature required for bit formation.

Errors in the analysis of bit writing originate from four sources: modeling error for the thermal conductivity of the tip, differences between tabulated properties for bulk PMMA and the actual properties of PMMA in an ultrathin film, errors in modeling the value of  $F_{pl}$ , and numerical errors. The most significant errors are modeling errors, in which the simple modeling approach does not accurately capture all of the relevant physics. The phonon scattering model induces a temperature error of 15% through the assumption of constant  $Cv$  and additionally induces a temperature error of 5% in the interface resistance model. Errors in  $F_{pl}$  origi-

nate from the approximate polymer flow model and from unknown property values. The sum of these errors yields a total error of +7% / -22% in time and +6% / -23% in temperature. Figure 4 shows the overall error of the present modeling approach through error bars on the smooth prediction curves.

## Conclusions

This paper describes simple modeling of the time, temperature, and force required to form a data bit indentation with a heated silicon probe tip. The predictions compare well with data for a tip radius of 20 nm, a polymer layer thickness of 35 nm, and a range of loading force, time, and heating temperature. The modeling and simulation approach and results could be used to improve writing rate and data density of thermomechanical data storage device. One possible improvement in the cantilever design would be to increase the cantilever resonance frequency while preserving the cantilever spring constant, which would allow high loading forces and improved cantilever mechanical response time. Improved experiments that carefully track the physical parameters present in thermomechanical data storage would motivate a more rigorous study of heat flow in the cantilever tip and polymer mass transport. The appropriate simulations would then consider the phonon radiation problem in the tip and the full flow field in the polymer.

## Acknowledgment

The authors are grateful for extensive technical exchanges and support from the Micro/NanoMechanics Group at the IBM Zurich Research Laboratory.

## Nomenclature

$d$	= local tip diameter
$d_{\text{contact}}$	= diameter of tip-polymer contact
$k$	= thermal conductivity of tip
$k_{\text{cant}}$	= spring constant of cantilever
$r_{\text{tip}}$	= tip radius of curvature
$t_{\text{pl}}$	= thickness of melted polymer
$v$	= average phonon velocity
$x$	= vertical tip position
$C$	= heat capacity of the silicon cantilever tip
$F_{\text{load}}$	= tip loading force
$F_{\text{pl}}$	= force with which polymer resists tip penetration
$G$	= polymer shear modulus
$R_{\text{contact}}$	= tip-polymer thermal contact resistance
$R_{\text{spread}}$	= thermal spreading resistance in polymer
$\chi$	= Poisson's ratio in polymer
$\eta_{\text{pl}}$	= polymer viscosity
$\Lambda$	= phonon mean free path

## References

- [1] Vettiger, P., Cross, G., Despont, M., Drechsler, U., Duerig, U., Gotsmann, B., Haberle, W., Lantz, M., Rothuizen, H., Stutz, R., and Binnig, G., 2002, "The "Millipede"-Nanotechnology Entering Data Storage," *IEEE Trans. Nanotechnol.*, **1**, pp. 39–64.
- [2] Vettiger, P., Despont, M., Drechsler, U., Dürig, U., Haberle, W., Lutwyche, M. I., Rothuizen, H. E., Stutz, R., Widmer, R., and Binnig, G. K., 2000, "The "Millipede"-More Than One Thousand Tips for Future AFM Data Storage," *IBM J. Res. Dev.*, **44**, pp. 323–340.
- [3] Binnig, G., Despont, M., Drechsler, U., Haberle, W., Lutwyche, M., Vettiger, P., Mamin, H. J., Chui, B. W., and Kenny, T. W., 1999, "Ultrahigh-Density Atomic Force Microscopy Data Storage With Erase Capability," *Appl. Phys. Lett.*, **76**, pp. 1329–1331.
- [4] Chui, B. W., Stowe, T. D., Ju, Y. S., Goodson, K. E., Kenny, T. W., Mamin, H. J., Terris, B. D., and Ried, R. P., 1998, "Low-Stiffness Silicon Cantilever With Integrated Heaters and Piezoresistive Sensors for High-Density Data Storage," *J. Microelectromech. Syst.*, **7**, pp. 69–78.
- [5] Weber, L., Gmelin, E., and Queisser, H. J., 1989, "Thermal Resistance of Silicon Point Contacts," *Phys. Rev. B*, **40**, pp. 1244–1249.
- [6] Phelan, P. E., Nakabepu, O., Itoh, K., Hijikata, K., Ohmori, T., and Torikoshi, K., 1993, "Heat Transfer and Thermoelectric Voltage at Metallic Point Contacts," *J. Heat Transfer*, **115**, pp. 757–762.
- [7] Shi, L. and Majumdar, A., 2002, "Thermal Transport Mechanisms at Nanos-

- cale Point Contacts," *J. Heat Transfer*, **124**, pp. 329–337.
- [8] Nakabeppu, O., Igeta, M., and Hijikata, K., 1997, "Experimental Study on Point-Contact Transport Phenomena Using the Atomic Force Microscope," *Microscale Thermophys. Eng.*, **1**, pp. 201–213.
- [9] Lutwyche, M. I., Despont, M., Drechsler, U., Durig, U., Hablerle, W., Rothuizen, H., Stutz, R., Widmer, R., Binnig, G. K., and Vettiger, P., 2000, "Highly Parallel Data Storage System Based on Scanning Probe Arrays," *Appl. Phys. Lett.*, **77**, pp. 3299–3301.
- [10] Chui, B. W., Asheghi, M., Ju, Y. S., Goodson, K. E., Kenny, T. W., and Mamin, H. J., 1999, "Intrinsic-Carrier Thermal Runaway in Silicon Microcantilevers," *Microscale Thermophys. Eng.*, **3**, pp. 217–228.
- [11] Mark, J. E., 1999, *Polymer Data Handbook*, Oxford University Press, New York.
- [12] Sverdrup, P. G., Ju, Y. S., and Goodson, K. E., 2001, "Sub-Continuum Simulations of Heat Conduction in Silicon-on-Insulator Transistors," *J. Heat Transfer*, **123**, pp. 130–137.
- [13] Masters, N., Ye, W., and King, W. P., 2005, "The Impact of Sub-Continuum Gas Conduction on the Sensitivity of Heated Atomic Force Microscope Cantilevers," *Phys. Fluids*, **17**, p. 100615.
- [14] Schwartz, E. T., and Pohl, R. O., 1989, "Thermal Boundary Resistance," *Rev. Mod. Phys.*, **61**, pp. 605–668.
- [15] Ziman, J. M., 1960, *Electrons and Phonons*, Oxford University Press, Oxford.
- [16] Casimir, H. B. G., 1938, "Note on the Conduction of Heat in Crystals," *Physica (Amsterdam)* **5**, pp. 495–500.
- [17] Kittel, C., 1996, *Introduction to Solid State Physics*, 7th ed., Wiley, New York.
- [18] Touloukian, Y. S., 1970, *Thermal Conductivity: Nonmetallic Solids*, IFI/Plenum, New York.
- [19] Cappella, B., and Dietler, G., 1999, "Force-Distance Curves by Atomic Force Microscopy," *Surf. Sci. Rep.*, **43**, pp. 1–104.
- [20] Sneddon, I. N., 1965, "The Relation Between Load and Penetration in the Axisymmetric Boussinesq Problem for a Punch of Arbitrary Profile," *Int. J. Eng. Sci.*, **3**, pp. 47–57.
- [21] King, W. P., Kenny, T. W., Goodson, K. E., Cross, G. L. W., Despont, M., Durig, U. T., Rothuizen, H., Binnig, G., and Vettiger, P., 2002, "Design of Atomic Force Microscope Cantilevers for Combined Thermomechanical Writing and Thermal Reading in Array Operation," *J. Microelectromech. Syst.*, **11**, pp. 765–774.
- [22] Roshenow, W. M., and Choi, H. Y., 1961, *Heat, Mass, and Momentum Transfer*, Prentice-Hall, Englewood Cliffs, NJ.
- [23] Sheehan, P. E., Whitman, L. J., King, W. P., and Nelson, B. A., 2004, "Nanoscale Deposition of Solid Inks via Thermal Dip Pen Nanolithography," *Appl. Phys. Lett.*, **85**, pp. 1589–1591.
- [24] Nelson, B. A., King, W. P., Laracuate, A., Sheehan, P. E., and Whitman, L. J., 2006, "Direct Deposition of Continuous Metal Nanostructures by Thermal Dip-Pen Nanolithography," *Appl. Phys. Lett.*, **88**, p. 033104.
- [25] King, W. P., 2005, "Design Analysis of Heated Atomic Force Microscope Cantilevers for Nanotopography Measurements," *J. Micromech. Microeng.*, **15**, pp. 2441–2448.
- [26] King, W. P., Kenny, T. W., and Goodson, K. E., 2004, "Comparison of Thermal and Piezoresistive Sensing Approaches for Atomic Force Microscopy Topography Measurements," *Appl. Phys. Lett.*, **85**, pp. 2086–2088.
- [27] Cross, G., Despont, M., Drechsler, U., Dürig, U., Vettiger, P., King, W. P., and Goodson, K. E., 2001, "Thermomechanical Formation and Thermal Sensing of Nanometer-Scale Indentations in PMMA Thin Films for Parallel and Dense AFM Data Storage," *Mater. Res. Soc. Symp. Proc.*, **649**, pp. Q2.3.1–Q2.3.7.
- [28] Ferry, J. D., 1980, *Viscoelastic Properties of Polymers*, Wiley, New York.
- [29] Fuchs, K., Friedrich, C., and Weese, J., 1996, "Viscoelastic Properties of Narrow-Distribution Poly(methyl methacrylates)," *Macromolecules*, **29**, pp. 5893–5901.
- [30] Deen, W. M., 1998, *Analysis of Transport Phenomena*, Oxford University Press, New York.
- [31] Terris, B. D., Rishton, S. A., Mamin, H. J., Ried, R. P., and Rugar, D., 1998, "Atomic Force Microscope-Based Data Storage: Track Servo and Wear Study," *Appl. Phys. A: Mater. Sci. Process.*, **66**, pp. S809–S813.
- [32] Mamin, H. J., Ried, R. P., Terris, B. D., and Rugar, D., 1999, "High-Density Data Storage Based on the Atomic Force Microscope," *Proc. IEEE*, **87**, pp. 1014–1027.